



Numerical Optimization of *basic* and *finned* Counter-Flow Dehumidifier with *adiabatic* and *convective* boundary conditions coupled with Thermo-Electric Cooler (TEC)

Adem H. Ibrahim

Engineering Department, Norfolk State University, Norfolk, Virginia, USA

Email: ahibrahim@nsu.edu

Abstract

A counter-flow dehumidifier *with* and *without* uniform rectangular fins was connected to a generic thermoelectric cooler to optimize for optimum water extraction and air dehumidification. To qualitatively analyze the humidifier's performance, adiabatic and convective boundary conditions on the fins' tips were implemented. Temperature of the cold face of the thermo couple was kept lower than that of ambient temperature of air so that temperature gradient is formed on the cold side. In this way the incoming air saturates and condenses on the cold surface of the thermoelectric cooler. The heat (Q_L) at temperature T_{SC} , accumulated on the cold side is pumped to the hot side at temperature T_{SH} . The heat, Q_H , on the hot side must be continuously expelled by the electric power provide by the thermoelectric couple through Peltier effect. To accomplish this, a counter flow cool air is fed to the hot face of the thermoelectric cell. The numerical analysis indicates that augmenting the dehumidifier with a number of fins just for a small amount of electric power input produces a better amount of water and dehumidifies the incoming air at a faster rate as compared to the dehumidifier without fins. Eventhough the convective boundary conditions exhibits slightly better performance index as compared to the adiabatic boundary condition, both boundary conditions resulted in almost identical temperature distributions and mass production.

Key words: fin effectiveness, fin efficiency, fins, thermoelectric cooler, saturation humidity ratio.

Introduction

A vast range of thermoelectric materials have been investigated for a wide range of applications [Refs.1-6]. As a result of their versatility and simplicity, many researchers have delved into optimizing their efficiencies [refs.1, 2, 3, 8, 9 and 10]. A common Thermo-Electric heat pump [Figs.1&2] which is commercially available is considered to dehumidify

moist air in conjunction with production of potable water. The dehumidification and collection of potable water is enhanced by incorporating an optimum number of fins. This technique of dehumidification and collection of drinking water is most valuable in places where hot and muggy/humid weather is common. The counter flow heat exchanger with fins [Fig. 3,] is represented by two counter flow channels whereby warm air pumped in on one side and cooled air on the other side. In the middle of the channel sits the Thermo-Electric Couple [Fig.1 & 2] whose cold face with temperature, T_{SC} , is exposed to the ambient and humidity ratio of T_i and ω_i , respectively. The cold surface temperature, T_{SC} is kept lower than the incoming ambient temperature, T_i , so that condensation takes place to produce water (refs. 10 and 11). An electric power input is provided to the thermo-electric cell [Fig. 2] so that the cold side heat, \dot{Q}_L , which has temperature, T_{SC} , is pumped to the hot side of the thermo-Electric element with heat, \dot{Q}_H , and of temperature, T_{SH} .

In order to study the viability of Thermo-Electric heat pump for this purpose, optimization and analysis is carried out using multiple fins with different temperature scales. For the counter flow heat exchanger [Fig. 3], the first and second laws of Thermodynamics analysis are used. Thereafter, an analytical closed form expression of the temperature distributions and humidity or vapor equations are derived. This process is simplified by using the analogy between heat and mass transfer on the wet/cold side of the Thermo-electric element. Since the cold side temperature of the element is lower than the incoming dew point temperature of the air, condensation of water vapor takes place on the cold side of the element. Also, the saturation humidity ratio of the cold side, ω_{SC} , is kept lower than the incoming air humidity, ω_i . As a consequence of this humidity difference, mass transfer occurs from the incoming air to the cold side of the thermo-Electric element [Refs. 1,2 and 3].

Geometric Descriptions and various areas computations of the rectangular fins are provided in Reference 2.

Heat transfer analysis of rectangular finned with uniform cross-sectional area:

The task of a fin is to extract heat from the body it is attached to and expel the heat from its own exposed surface to the surrounding medium via a convection mechanism. Using energy

balance, the quantity of heat conducted and convected by the finis derived from a differential element of the fin [Ref. 2] as:

$$\dot{Q}_x = \dot{Q}_{x+\Delta x} + dQ_{conv} + \dot{Q}_{TEC} \quad (1)$$

Where, \dot{Q}_{TEC} is the heat generated by the TEC and is obtained from the manufacture's data.

Eq. (1) is furthermore decoded by using Fourier's law for conduction and Newton's law for the convection:

$$\dot{Q}_x = -kA_c \frac{d[T(x) - T_\infty]}{dx} \quad (2)$$

$$\dot{Q}_{x+\Delta x} = -kA_c \frac{d[T(x) - T_\infty]}{dx} - k \frac{d}{dx} \left[A_c \frac{d[T(x) - T_\infty]}{dx} \right] \quad (3)$$

$$dQ_{conv} = h[T(x) - T_\infty]dA_s \quad (4)$$

Note that the differential circumferential surface area is:

$$dA_s = p dx \quad (5)$$

Where p is the perimeter of the fin.

Inserting Eqs. (2)through(5) into Eqn. (1) and considering constant cross-sectional area of the rectangular fin, one obtains the following heat equation:

$$\frac{d^2[T(x) - T_\infty]}{dx^2} - \left(\frac{hp}{kA_c} \right) \frac{d[T(x) - T_\infty]}{dx} + \frac{\dot{Q}_{TEC}}{k} = 0 \quad (6)$$

Eq. (5) can be further simplified using the following parameters:

$$\theta(x) = T(x) - T_\infty \quad m^2 = \frac{hp}{kA_c} \quad (7)$$

$$\frac{d^2\theta(x)}{dx^2} - m^2 \frac{d\theta(x)}{dx} + \frac{\dot{Q}_{TEC}}{k} = 0 \quad (8)$$

Eq. (8) is a linear second order ordinary differential equation with constant coefficients and its solution can be obtained by inserting the Eigen value function for boundary value problem as provided in ref [2]. Here, we only provide the relevant governing equations both for the adiabatic and convective boundary conditions.

A case with finite length:

$$\theta(x) = \theta_b \frac{\frac{e^{m(l-x)} + e^{-m(l-x)}}{2}}{\frac{e^{ml} + e^{-ml}}{2}} = \theta_b \frac{\cosh[m(l-x)]}{\cosh(ml)} \quad (9)$$

$$\text{Where: } \theta(x)|_{x=0} = \theta_b = T_b - T_\infty \quad (10)$$

The case with infinite fin length:

$$\theta(x \rightarrow \infty) = \theta_b e^{-mx} \quad (11)$$

Considered Fin Boundary conditions

In order to get a simplified expression for Eq. (8) as applied to fins, we need to determine three boundary conditions dictated by the flow field physics, namely at base and tip of the fin. As provide by Eqn. 9, the **first boundary** condition will be the temperature at that base cross-sectional area of the fin.

$$\theta(x)|_{x=0} = \theta_b = T_b - T_\infty \quad (12)$$

The **second boundary** condition we consider is the **adiabatic** conditions at the fin tip. This condition assumes that the convective heat transfer at the fin's tip is negligible due to the fact that the tip area extremely small and hence it can be considered as if there is no rate of heat transfer from the fin tip:

$$\text{temperature gradient} = \left. \frac{d\theta(x)}{dx} \right|_{x=l} = 0 \quad (13)$$

Following the method provided in Ref. [2], one needs to compensate for the negligible convection from the fin tip. Hence, the following corrections are adopted for the following parameters:

$$l_c = l + \frac{t}{2} \quad (14a)$$

$$\frac{p_c}{A_c} \cong \frac{2}{t} \quad (14b)$$

$$m_c = \sqrt{\frac{h}{k} \frac{p}{A_{c_fin}}} = \sqrt{\frac{2}{t} \frac{h}{k}} \quad (14c)$$

Applying Eqs.(12) and (13)to the heat distribution given by eq. (9), the **adiabatic rate of heat conduction** at the base of the fin will assume the form of:

$$q_{\text{adiabatic_fin_tip}} = \dot{Q}_{\text{adiabatic_fin_tip}} = -kA_c \left. \frac{d\theta(x)}{dx} \right|_{x=0} = \sqrt{khpA_c} \theta_b \tanh(ml) \quad (15)$$

The **third boundary** we are considering is the **convective heat transfer** from the fin's tip.

In this scenario, the rate of heat conduction from the fin's body has to be equal to the rate of heat convected the fin tip, hence:

$$-kA_c \left. \frac{d[T(x) - T_\infty]}{dx} \right|_{x=l} = hA_c [T(x) - T_\infty]_{x=l} \quad (16)$$

$$\text{Define: } \alpha = \frac{km}{h} \quad (17)$$

Following the derivation from Ref [2], one obtains:

a) Temperature distribution:

$$\frac{\theta(x)}{\theta_b} = \frac{\cosh[m(l-x)] + \frac{1}{\alpha} \sinh[m(l-x)]}{\cosh(ml) + \frac{1}{\alpha} \sinh(ml)} \quad (18)$$

b) Using equations (16 and 18), the rate of heat transfer for a fin with convective tip is:

$$\dot{Q}_{convective_tip} = -kA_c \left. \frac{d[T(x) - T_\infty]}{dx} \right|_{x=0} = \sqrt{kh p A_{c_fin}} \theta_b \frac{\frac{1}{\alpha} \cosh(ml) + \sinh(ml)}{\cosh(ml) + \frac{1}{\alpha} \sinh(ml)} \quad (19)$$

Determination of an optimum fin length for adiabatic boundary condition:

The proper length of a fin for an adiabatic fin tip is determined by comparing the adiabatic rate of heat transfer with the rate of heat transfer for an infinite length. Hence:

$$\frac{\dot{Q}_{adiabatic}}{\dot{Q}_{l \rightarrow \infty}} = \frac{\sqrt{kh p A_c} * \theta_b * \tanh(ml)}{\sqrt{kh p A_c} * \theta_b} = \tanh(ml) \quad (20a)$$

Following the Ref. [2], one gets:

$$l_{opt} = \frac{5}{m} \quad (20b)$$

With the reduction of ml by 50%, one will just compromise a 1% lose of heat transfer and the optimum length can be further approximated by:

$$l_{opt_mod} = \frac{2.5}{m} \quad (20c)$$

Fin Performance:

With corrected dimensions, the performance of a fin is evaluated by determining its efficiency and effectiveness as follows:

Fin efficiency:

a) Using Eq. (15) for adiabatic flow condition:

$$\eta_{adiabatic} = \frac{\dot{Q}_{fin}}{\dot{Q}_{max}} = \frac{\dot{Q}_{fin}}{hA_{fin_surface_area}(T_b - T_{\infty})} = \frac{\sqrt{kh p A_{fin_surface_area}} \theta_b \tanh(m_c l_c)}{hA_{fin_surface_area} \theta_b} = \frac{\tanh(m_c l_c)}{m_c l_c} \quad (21)$$

b) Using Eq. (19) for convective low condition:

$$\eta_{convective} = \frac{\dot{Q}_{fin}}{\dot{Q}_{max}} = \frac{\dot{Q}_{fin}}{hA_{fin_surface_area}(T_b - T_{\infty})} = \frac{\sqrt{kh p A_{fin_surface_area}} \theta_b \frac{\frac{1}{\alpha} \cosh(ml) + \sinh(ml)}{\cosh(ml) + \frac{1}{\alpha} \sinh(ml)}}{hA_{fin_surface_area} \theta_b} = \frac{\frac{1}{\alpha} \cosh(ml) + \sinh(ml)}{\cosh(ml) + \frac{1}{\alpha} \sinh(ml)} \quad (22)$$

Fin Effectiveness:

The main purpose of fins is to accelerate heat removal from the body they are attached to. If the fins are not properly dimensioned, numbered and positioned, they may contribute more resistance to heat conduction and may hamper to the heat removal effort from the heat pump. Therefore, the effectiveness, (ε_{fin}) , of fins for the better removal of heat or cooling and thereby condensing it water is decided by finding the ratio of convective heat removed by the fin surface area to the convective heat removed from the heat pump surface without the fin attached to it. It is generally accepted to incorporate fins if the efficiency ratio is greater or equal to 2. Hence:

$$\varepsilon_{fin} = \frac{\dot{Q}_{fin_surf}}{\dot{Q}_{no_fin}} = \frac{\dot{Q}_{fin_surf}}{hA_{fin_base}(T_b - T_{\infty})} = \frac{\dot{Q}_{fin_surf}}{hA_{fin_base} \theta_b} = \frac{\eta_{fin} \dot{Q}_{fin_max}}{hA_{fin_base} \theta_b} = \frac{\eta_{fin} hA_{fin_surf} \theta_b}{hA_{fin_base} \theta_b} = \eta_{fin} \frac{A_{fin_surf}}{A_{fin_base}} \quad (23)$$

$$\varepsilon_{fin_tot} = \frac{\dot{Q}_{tot_fin_surf}}{\dot{Q}_{no_fin}} = \frac{\dot{Q}_{tot_fin_surf}}{hA_{fin_base}(T_b - T_{\infty})} = \frac{h[A_{no_fin} + \eta_{fin} A_{fin_surf}] \theta_b}{hA_{fin_base} \theta_b} = \frac{A_{no_fin} + \eta_{fin} A_{fin_surf}}{A_{fin_base}} \quad (24)$$

Where the various areas are provided by Ref. [2]. \dot{Q}_{fin_surf} is the fin's heat transfer rate associated with one of the boundary condition provided.

a) Using Eqs. (19a, b and c), the fin's effectiveness with adiabatic fin tip with corrected dimensions can be shown to be:

$$\varepsilon_{fin_adiabatic} = \frac{\sqrt{khpA_{c_fin_base}} \theta_b \tanh(m_c l_c)}{hA_{c_fin_base} \theta_b} = \sqrt{\left(\frac{k}{h}\right) \left(\frac{p}{A_{c_fin_base}}\right)_{corrected}} \tanh(m_c l_c) \quad (25)$$

b) Using Eqs. (19a, b, and c), the fin effectiveness with convective fin tip will be:

$$\varepsilon_{fin_convective} = \frac{\sqrt{khpA_{c_fin_base}} \theta_b \frac{1}{\alpha} \cosh(ml) + \sinh(ml)}{hA_{c_fin_base} \theta_b \cosh(ml) + \frac{1}{\alpha} \sinh(ml)} = \sqrt{\left(\frac{k}{h}\right) \left(\frac{p}{A_{c_fin_base}}\right)_{corrected}} \frac{\frac{1}{\alpha} \cosh(ml) + \sinh(ml)}{\cosh(ml) + \frac{1}{\alpha} \sinh(ml)} \quad (26)$$

Determination of condensed liquid water on the cold side of the element:

The details of Liquid mass, humidity and temperature derivations and as well as computations are follows:

Mass flow rate:

$$\dot{m}_{air} = \rho_{air_humid} u_{\infty} A = \rho_{air_humid} u_{\infty} wL [kg / sec] \quad (27)$$

Humidity:

$$\omega_i - \omega_L = (\omega_i - \omega_{sc}) \left[1 - e^{-a\sqrt{L}} \right] \quad (28a)$$

Letting,

$$a = \frac{0.664 * \rho * D_{va} Sc^{\frac{1}{3}}}{\dot{m}_{air_humid}} \sqrt{\frac{u_{\infty}}{\nu}}$$

(28b)

Taking into account the flow analysis with fins, the parameter a, must be modified as:

$$a_{fin} = a + a \left(\eta_{fin} * \frac{A_{fin}}{A_{b=c=no_fin}} \right) \quad (28c)$$

From Eq. (27), the condensed mass of liquid is equivalent to the mass of water vapor lost by the air due to condensation. Then, integrating Eq. (27) the over length, L, of the Thermo-Electric cell and using Eqs. (31), the liquid mass is:

$$\dot{m}_l = -\dot{m}_{air_humid}(\omega_L - \omega_i) = \dot{m}_{air_humid}(\omega_i - \omega_L)$$

(29)

The temperatures on cold and hot sides of the Thermo-Electric element:

The sensible heat transferred from the cold side is equal to the heat conducted across the channel to the hot side of the thermo-Element.

$$d\dot{Q} = Ah(T - T_{SC}) = \dot{m}_{air_humid}c_p dT$$

(30)

a) Using Eq. (32), the temperature on the cold side of TEC will be:

$$(T_{x=L} - T_i)_{cold_face} = [T_i - T_{SC}] [e^{-b\sqrt{L}} - 1]$$

(31)

b) In the same way, the temperature distribution on the hot face is:

$$(T_{x=L} - T_i)_{ho_face} = [T_{SH} - T_i] [1 - e^{b\sqrt{L}}]$$

(32a) and letting:

$$b = \frac{-0.664 * k}{\dot{m}_{air} c_p} * Pr^{\frac{1}{3}} * \sqrt{\frac{u_{\infty}}{\nu}}$$

(32b)

In analysis with fins, the parameter b in the heat and temperature computations must be modified as:

$$b_{fin} = b + b \left(\eta_{fin} * \frac{A_{fin}}{A_{b=c=no_fin}} \right)$$

(32c)

The performance data of the thermoelectric pump is provided by the manufacturer Ref. [6] by figure 2 as:

$$\dot{Q}_{H_TEC} = A + B * (T_{SH} - T_{SC})$$

(33)

$$\dot{Q}_{L_TEC} = C + D * (T_{SH} - T_{SC})$$

(34)

where A, B, C and D are constants that are determined from the removed and absorbed heat graphs[Fig. 2].

Numerical Optimization Procedure:

As provided by equations (33) and (34), the salient characteristics of the thermoelectric module [Fig. 1] were computed by linear interpolation from the graphs [fig. 2]. The heat pump is considered to be one meter in height and 0.02 meter deep. To initiate the numerical optimization, the incoming ambient temperature and humidity values are predicted. One must be cognizant that, for the condensation to take place on the cold face, the ambient temperature and humidity need to be higher than the temperature and humidity on the cold surface. Since the temperatures on the hot and cold sides of the thermo couple are unknown a priori, iterative method is adopted as presented in reference 1.

Numerical optimization results:

Using the converged values, the liquid mass rate, Eq. (46), is computed to be 29.387 kg/hour. Along with the condensed mass of condensed liquid, the converged values of humidity and temperatures are shown on Tables 2 and 3.

The analysis for the TEC with fins indicates that once the condensation is completed and the heat is removed from the hot face of the couple, the temperature on the hot side subsides from 47.2401 degrees to 43.4707 degrees Celsius. As reported in reference 1, the temperature on hot side without fins was 85.6599 degrees Celsius and reached to 48.9629 degrees Celsius after the condensation is completed. The numerical experimentation shows that inclusion of fins speeds up the de-humidification process thereby increasing the amount of water collected from 2.53 kg/hr. to 29.387 kg/hr. [Tables 2]. In Tables 4 and 5, the temperatures and rate of heat both on the hot and cold sides produced are presented. As the result of the fins' inclusion, one can observe from these tables that the temperature quickly draws down while the amount of heat removed or condensed increases likewise. Consequently, the process of de-humidification ensues fast and the amount of water accumulation increases dramatically.

Figs. 1-3 describe the feature, characteristics and arrangement of the Thermo-Electric Couple (TEC) for the dehumidification process. Figs. 4-6 describe the fin's geometric characteristics and fin array arrangement. The number of fins used in this analysis is 40 and their dimensions are provided in table 1.

Conclusion:

A thermoelectric device was used to serve dual purposes, namely to cool the incoming air and produce water. In doing so, the air is dehumidified resulting in comfort that can be useful in places where humidity is extremely high. To increase the efficiency and the amount of potable water collected by the thermocouple, fins were incorporated. The analysis with the incorporation of fins to the Thermo-Electric couple shows that the temperature on both sides

of the TEC goes down and the water accumulation quickly gets higher. As presented in Table 3, the fin efficiency reaches to 92% whereas the effectiveness gets to 3.19. To get a full scope of the analysis, we recommend that Computational Fluid Dynamics needs to be used so that one can fully analyze the interaction of TEC and fins with the flow field.

TEC height	1.0 [m]
TEC width	0.02 [m]
Fin length	0.05 [m]
Fin width	0.02 [m]
Fin thickness	0.005 [m]
Fin gap	0.05 [m]
Total number of fins	40 (calculated using fin gap and TEC length)

Table 1: TEC and fin dimension specification

Fin	Boundary condition	\dot{m}_{liquid} $\left[\frac{kg}{hr}\right]$	$\omega_{x=L}$ $\left[\frac{kg_{H_2O}}{kg_{dry_air}}\right]$	T_{SH} $[^{\circ}C]$	T_{SC} $[^{\circ}C]$	$T_{x=L}$ $[^{\circ}C]$	Fin efficiency	Fin effectiveness
Non	basic	2.53152	0.056222	48.9629	33.5555	42.7058	-	-
Yes	adiabatic	29.387	0.0158525	43.4707	30.8292	34.0976	0.920474	3.14777
Yes	convective	29.8239	0.015195	43.4629	30.8241	33.9574	0.951238	3.21956

Table 2: Optimum values at x=L with adiabatic and convective boundary conditions [Refs. 1&2].

X[m]	TSH[Celsius]	TSC[Celsius]	Q_dot_H[kwatts]	Q_dot_L[kwatts]
0.005	85.6599	37.3002	0.0367654	0.00617589
0.1	60.139	38.5276	0.0658227	0.0306745
0.2	55.5834	36.5921	0.0681536	0.0326397
0.3	53.4543	35.642	0.0691974	0.0335198
0.4	52.1523	35.0482	0.0698233	0.0340474
0.5	51.2497	34.6311	0.070252	0.0344089
0.6	50.576	34.317	0.0705693	0.0346764
0.7	50.0481	34.0692	0.0708164	0.0348847
0.8	49.6198	33.8672	0.0710159	0.0350529
0.9	49.2632	33.6982	0.0711813	0.0351924
0.999	48.9629	33.5555	0.0713201	0.0353094

Table 3: Temperature and heat distributions along the cold and hot faces of the thermocouple **withoutfins**[Ref. 1].

X[m]	TSH[Celsius]	TSC[Celsius]	Q_dot_H[kwatt]	Q_dot_L[kwatt]
0.005	47.2401	32.7275	0.0722536	0.0360964
0.1	44.0791	31.1634	0.0735122	0.0371576
0.2	43.8123	31.0237	0.0736254	0.037253
0.3	43.6956	30.9606	0.0736728	0.0736728
0.4	43.627	30.9224	0.0736997	0.0373157
0.5	43.5809	30.896	0.0737171	0.0373304
0.6	43.5473	30.8763	0.0737294	0.0373407
0.7	43.5216	30.8609	0.0737385	0.0373484
0.8	43.5012	30.8484	0.0737455	0.0373543
0.9	43.4845	30.838	0.073751	0.0373589
0.999	43.4707	30.8292	0.0737554	0.0373626

Table 4: Temperature and heat distributions along the cold and hot faces of the thermo-couple with **pins** and **convective boundary condition**.

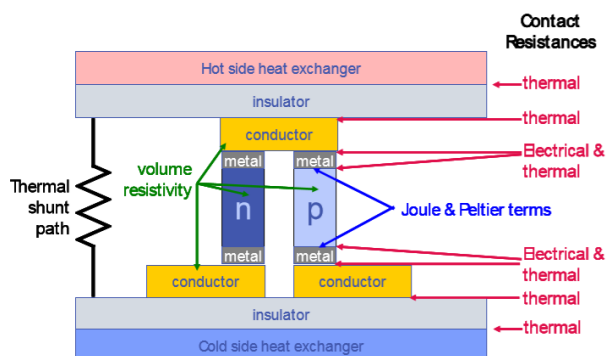


Fig. 1: General Feature of Thermoelectric Module [Ref. 6] (www.tetech.com)

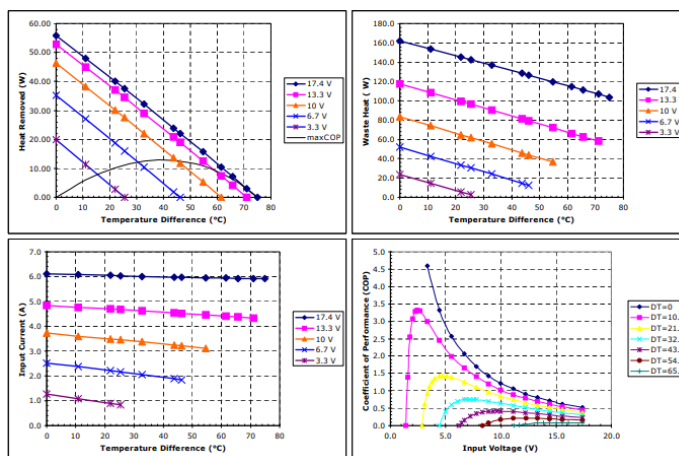


Fig. 2: Peltier-Thermoelectric Module chart [Ref. 6] (www.tetech.com)

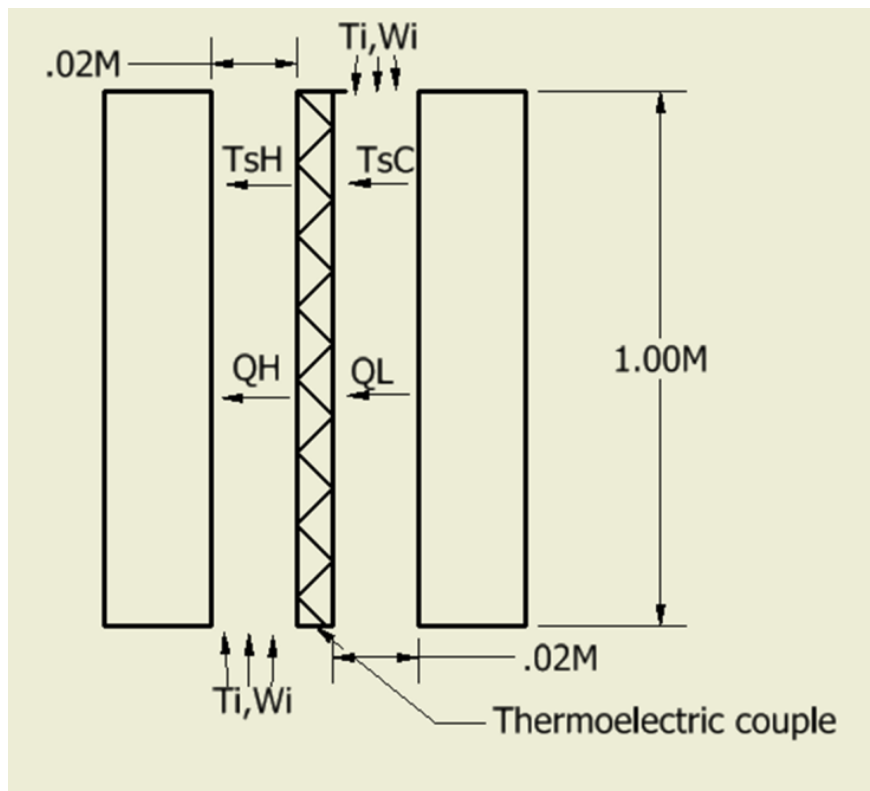


Fig. 3:Counter flow mechanism in Thermo-electric couple.

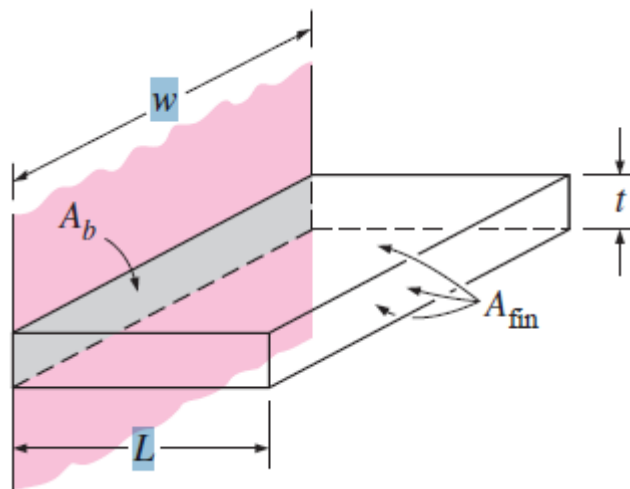


Fig.4: Fin geometry specification [Refs. 4 & 5]

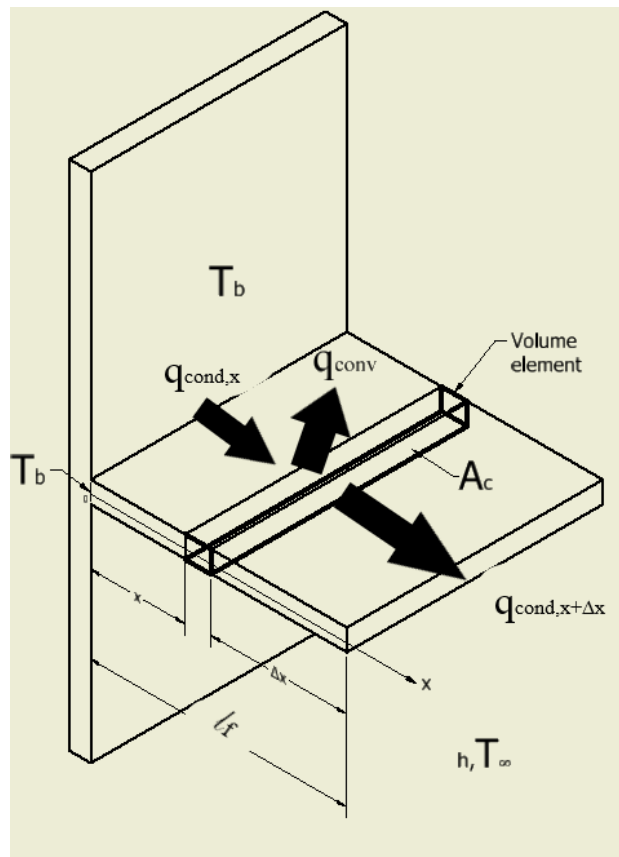


Fig. 5: Fin conductive and convective heat flow mechanism.

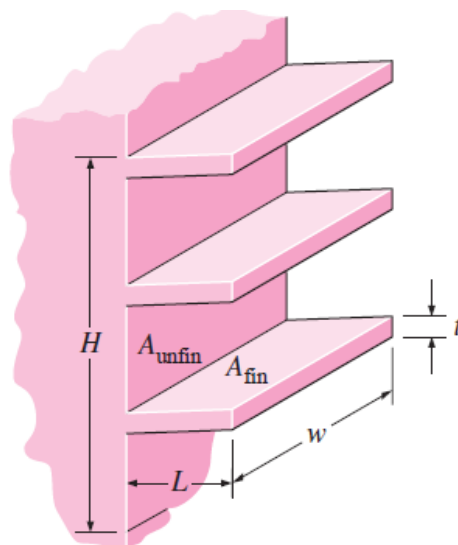


Fig. 6: Fin distribution along a thermo-electric height and fin area definition [Refs. 4 & 5]

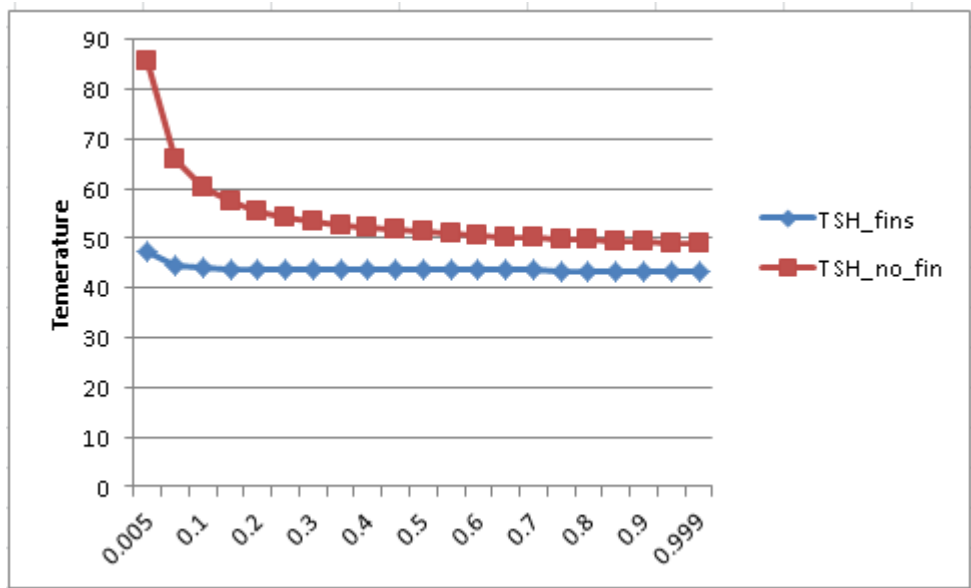


Fig. 7: Comparison of temperature distribution on the hot side of TEC.

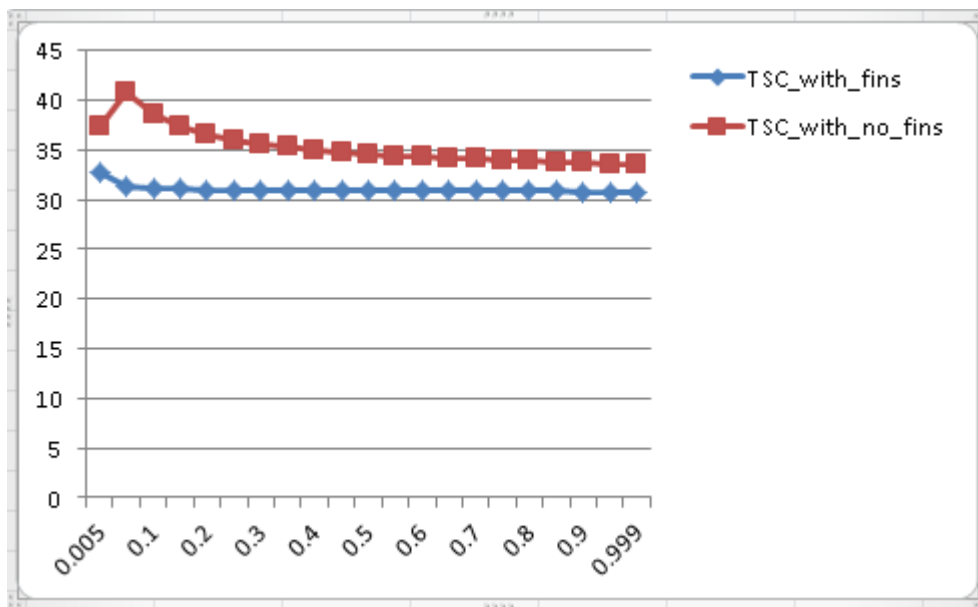


Fig. 8: Comparison of temperature distribution on the cold side of TEC.

References:

1. Adem H. Ibrahim," Optimization and Analysis of a Counter-Flow Dehumidifier with a Thermo-Electric Heat Pump", International Research Journal of natural and Applied Sciences, Volume 6, issue 12, December 2019.
2. Adem H. Ibrahim," Parametric Optimization of *finned* Counter-Flow Dehumidifier coupled with a Thermo-Electric Cooler (TEC)", International Research Journal of natural and Applied Sciences, Volume 8, issue 01, January 2021.

3. Xiabing Luo and etal., “Design Optimization of horizontally-located Plate Fin Heat-Sink for High power LED Street Lamps”, Electronic Components and Technology Conference, 2009, <http://www.paper.edu.cn>.
4. Yunus A. Cengel and Afshin J. Ghajar, “*Heat and Mass Transfer, Fundamental and Applications*”, Fifth edition, McGraw-Hill.
5. Theodor L. Bergman and etal, “*Fundamental of Heat Transfer*”, Seventh edition, Wiley.
6. Performance Chart Instructions, TE Technology, INC., <http://www.tetech.com>
7. Kogo, G., Lee, H., Ibrahim, A. H., Bo, X., Pradhan, S. K. and Bahoura, M. (2018), “Highly-efficient thermoelectric pn-junction device based on Bi₂Te_{1.8} and Molybdenum Disulfide (MoS₂) films fabricated by RF magnetron sputtering technique.” *Journal of Applied Physics* 124, 165106.
8. Al-Hababbeh, O.M., Mohammad, A., Al-Khalid, A., Khanfer, M. and Obeid, M., (February 8, 2016), “Design Optimization of a large-scale Thermoelectric Generator”, *Journal of King Saud University, Engineering Sciences*.
9. Dashevsky, Z., Gelbstein, Y., Edry, I., Drabkin, I., and Dariel, M. P. (2003), “Optimization of Thermoelectric Efficiency in Graded Materials”, 22nd International Conference on Thermoelectric, IEEE.
10. Lee, Gysou, Lee, Garam, Kim, C. S., Kim, Y. J., Choi, H., Kim, S., Kim, H. S., Lee, W. B. and Cho, B. J. (2017), “Material Optimization for Higher Power Thermoelectric Generator in Wearable Applications”, *Applied Sciences*, 7, 1015.
11. Montgomery, R. B. (1947), “Viscosity and Thermal conductivity of air and diffusivity of water vapor in air”, *Journal of Meteorology*, Vol. 4.
12. Lampinen, M., J. (Lecture Series), “*Thermodynamics of Humid Air*” (Translated by Juho Arjoranta).